

## **SIMULATION OF THE PENETRATION OF 6061-T6511 ALUMINUM ALLOY TARGETS BY OGIVE-NOSE RIGID PROJECTILES**

AHMAD MUJAHID AHMAD ZAIDI<sup>1</sup>

**Abstract.** An axisymmetric simulation model using mesh-less approach is developed to predict final penetration depth of 6061-T6511 aluminum alloy by rigid ogive-nose projectile. In this model, the target structures made of aluminium alloy are modelled by finite layers of aluminium alloy materials and the projectile is modelled by standard finite elements. Penetration resistance of the target structure is provided by functions derived from the principles of dynamic cavity expansion. Interaction between the finite elements and the mesh-less target model is made by applying penetration resistance load to the elements on the surface of the projectile nose. Final penetration depth results are compared with the experimental data. The simulation model shows good agreement with the experimental data.

*Keywords:* Penetration resistance, mesh-less treatment, ogive-nose, dynamic cavity expansion

### **1.0 INTRODUCTION**

Great demand exists for more efficient protection design to protect personals and critical components against impact by kinetic missiles, generated both accidentally and deliberately, in various impact and blast scenarios in both civilian and military activities. As a result, the study of impact resistance becomes essential in these applications. Numerous investigations have been performed to analyze impact resistance during impact process [1-4]. Due to the intricacy of the penetration mechanisms, investigations are generally based on experimental data. Conclusion of observations was then used to guide an engineering prediction model. Studies normally fall into three categories, i.e. empirical formulae based on data fitted, idealised analytical models based on physic laws and numerical simulations based on computational mechanics and material models.

Between the 70s and 90s, more empirical formulae were developed to satisfy the requirements from nuclear industries and analytical models which appeared in penetration prediction. Several empirical and analytical models have been successfully made for predicting penetration depth in various targets of materials [5-10]. During this period, numerical simulations were not reliable for penetration problems.

---

<sup>1</sup> School of Mechanical, Aerospace and Civil Eng., The University of Manchester, P.O Box 88, Manchester, M60 1QD, United Kingdom.  
Email: A.Ahmad-zaidi@postgrad.manchester.ac.uk

In the last decade, both the computer capability and computational mechanics significantly progressed and were widely used. The changes of interest from empirical and analytical models to numerical simulation have become inevitable because of its efficiency, low cost and versatility. (e.g., it is difficult to use analytical models to predict the trajectory of a projectile and its penetrability in a practical problem).

Traditionally, penetration modeling in numerical simulation usually adapted the fully coupled analysis, i.e., both projectile and target are discrete in computational code. However, there are weaknesses in the fully coupled analysis simulation, which certain categories have to be considered in order to performing simulation analysis, i.e., failure criterion [4, 11], contact problem [4, 11], mesh distortion for the large deformation [12-15] and reliable material model [4, 11].

Since the deformation and kinetics of projectile influences the trajectory of projectile, Warren and Tabbara [16] introduced a new technique to simulate penetration event. The interaction between projectile and target model can be made by applying penetration resistance (provided from dynamic cavity function) to the elements on the outer surface of the projectile mesh, as shown in Figure 1.

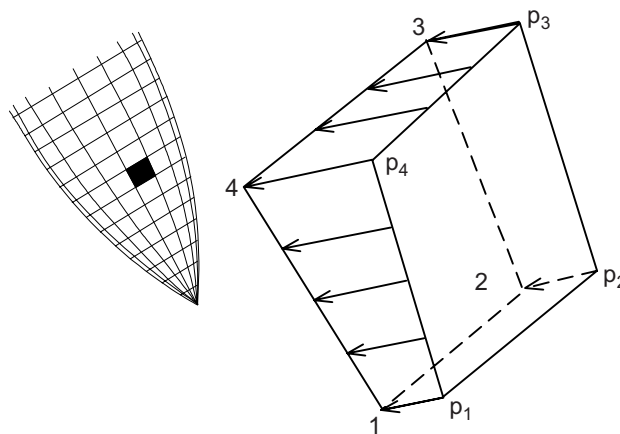


**Figure 1** Definition of a pressure boundary condition that acts on an element side [16]

In this paper, the concepts implemented by Warren and Tabbara [16] are applied in the ABAQUS finite element code for modeling penetration event. Simulation model is validated by comparing final penetration depth with experimental data obtained by Piewkutowski *et al.* [10].

## 2.0 MATERIAL PROPERTIES AND GEOMETRY

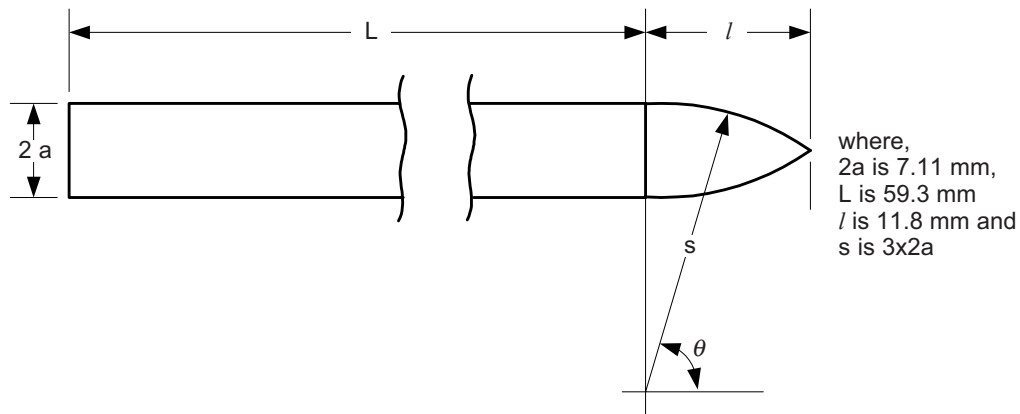
In this section, projectile is assume as a rigid body (non-deformable) with ogive nose and strikes the target at normal incidence. The material properties and the geometry

**Table 1** Material properties (Piewkutowski *et al.* [10])

	Material	Y (MPa)	A	B	$\rho(\text{Kg/m}^3)$	$\nu$
Projectile	Rigid	–	–	–	–	–
Target	6062-T6511 Al Alloy	276	5.0394	0.9830	2710	1/3

information for the simulation model are based on Piewkutowski *et al.* [10], as shown in Table 1 and Figure 2.

For ogive nose projectile, mass is 0.021 kg with 7.11 mm diameter and 71.1 mm long, as shown in Figure 2.

**Figure 2** Projectile geometry for ogive nose [10]

### 3.0 NUMERICAL SIMULATION

In this section, penetration event are modelled using ABAQUS finite element software package. The projectile is modelled in standard finite element with semi-spherical nose shape and treated as a discrete rigid body with element type RAX2. The aluminium alloy target is treated as a mesh-less by finite layers of aluminium alloy material, which impose penetration resistance on the projectile through resistance function based on dynamic cavity expansion theory (refer to Section 3.2). The resistance on the surface of rigid projectile is a function of the instantaneous velocity of projectile nose surface, which can be determined by the rigid motion of the projectile. Coupling between motion of rigid projectile and mesh-less target is made by exchanging the velocities and stresses through user-interfaces using FORTRAN95 software (refer to Section 3.3).

### 3.1 Mesh-less Treatment of the Target

In this method, the aluminum alloy target structure is described as a mesh-less. The resistance function which is based on dynamic cavity expansion theory is used to represent the penetration resistance of finite layered of aluminum alloy.

### 3.2 Penetration Resistance Function

The resistance load functions which have been derived from the principle of the dynamic cavity expansion can generally be represented in the following form [17]:

$$\sigma_n = AY + B\rho V_n^2 \quad [1]$$

where  $\sigma_n$  is the normal compressive stress representing the resistance load of the target structure and  $V_n$  is the normal expansion velocity.  $Y$  and  $\rho$  are yield stress and density of target material, respectively.  $A$  and  $B$  are dimensionless material constants. Those values (i.e,  $Y$ ,  $\rho$ ,  $A$  and  $B$ ) were shown in Table 1.

### 3.3 Explicit Dynamic Finite Element Algorithm in Simulation Model

The explicit dynamics analysis procedure is based upon the implementation of an explicit integration rule together with the use of diagonal or "lumped" element mass matrices. The equations of motion for the body (projectile) are integrated using the explicit central difference integration rule.

$$V^{(i+1/2)} = V^{(i-1/2)} + [(\Delta t^{(i+1)} + \Delta t^{(i)})/2]a^{[i]} \quad (2)$$

$$U^{(i+1)} = U^{(i)} + \Delta t^{(i+1)}V^{(i+1/2)} \quad (3)$$

where  $U$  is the displacement,  $V$  is the velocity and  $a$  is the acceleration. The superscript  $(i)$  refers to the increment number and  $(i-1/2)$  and  $(i+1/2)$  refer to mid-increment values. The central difference integration operator is explicit in that the kinematic state can be advanced using known values of  $V^{(i-1/2)}$  and  $a^{(i)}$  from previous increment. The computational efficiency of the explicit procedure depends on using the diagonal element mass matrices because of the inversion of the mass matrix that is used in the computation for the accelerations at the beginning of the increment is triaxial;

$$a^{(i)} = M^{-1}\Delta F \quad (4)$$

where are;

$$\Delta F = (F^{(i)} - I^{(i)}) \quad (5)$$

$$(F^{(i)} - I^{(i)}) = \sigma^{(i)}S \quad (6)$$

where  $M$  is the diagonal lumped mass matrix,  $S$  is the front nose's projectile surface,  $F$  is the applied force vector,  $I$  is the internal force vector and  $\sigma^{(i)}$  is determined by Equation (1).

#### 4.0 RESULTS AND DISCUSSION

In this section, results from simulations model are compared with experimental data [10]. Figure 5 represent pattern of the graph from Table 2.

**Table 2** Penetration depth data of Aluminum Alloy 6061-T6511.

Velocity(m/s)	Experimental(mm)	Simulation(mm)
569	58	67.1
570	55	67.3
679	72	87.9
821	102	115.2
966	140	142.3
1147	190	196.8

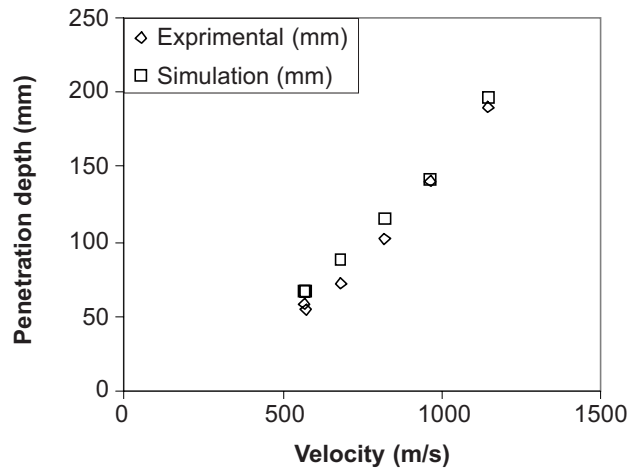


**Figure 3** Penetration depth against impact velocity

Table 2 and Figure 3 in Section 4.0 summarise the final penetration depths of projectiles obtained from simulation model and experimental data. Clearly, the simulation model gives an encouraging prediction, which follows the general trend of experimental results and offers an upper bound of experimental data. The reason simulation results produced upper bound of experimental data is due to rigid assumption that been made to the projectile. In addition, the rigid assumption of projectile model some how influence prediction results especially when impact velocity

is increased to the high velocity level, it will cause deformation on projectile and this will violates the rigid projectile assumption.

In simulation model, it is assumed that the projectile strikes target with normal incidents and there was no angle of obliquity during the process, i.e. the projectile model in simulations are constrained in the  $x$  and  $z$  directions, allowing it to move only in the  $y$  direction. However, in the real situation, projectiles experienced changes of yaw and pitch degree during trajectory [10], which may influence simulation predictions.

## 5.0 CONCLUSION

Simulations of the penetration of 6061-T6511 aluminum alloy target by rigid ogive nose projectile have been conducted in sequence to validate the experimental data obtained from Piewkutowski *et al.* [10] and verified cavity expansion functions to represent the target resistance in impact event. Encouraging predictions are observed when simulation results are compared to the experimental data.

## ACKNOWLEDGEMENTS

The author acknowledges the assistance and beneficial discussion with Dr. Q. M. Li and Mr. M. Z.Othman.

## NOMENCLATURE

$\sigma_n$	normal compressive stress, N/ m <sup>2</sup>
$\sigma^{(i)}$	compressive stress with incremental, N/ m <sup>2</sup>
$V_n$	normal expansion velocity, m/s
$Y$	yield stress, N/ m <sup>2</sup>
$\rho$	density of target material, kg/ m <sup>3</sup>
$A$ and $B$	dimensionless material constants.
$S$	front nose's projectile surface, m <sup>2</sup>
$U$	displacement, m
$a$	acceleration, m/s <sup>2</sup>
$(i)$	increment number
$M$	diagonal lumped mass matrix, kg
$F$	applied force vector, N
$I$	internal force vector, N
$\nu$	poisson ratio

## REFERENCES

- [1] Bishop, R. F., R. Hill, and N. F. Mott. 1945. The Theory of Indentation and Hardness Tests. *Proc Phys Soc.* 57(Part 3): 147-59.
- [2] Backman, M. E., and W. Goldsmith. 1978. The Mechanics of Penetration of Projectiles into Targets. *Int. J. Eng. Sci.* 16: 1-99.
- [3] Jonas, G. H., and J. A. Zukas. 1978. Mechanics of Penetration: Analysis and Experiment. *Int. J. Engng Sci.* 16: 879-904.
- [4] Anderson, C. E., Jr., and S. R. Bodner. 1988. Ballistic Impact: The Status of Analytical and Numerical Modeling. *Int. J. Impact Engn.* 7: 9-35.
- [5] Haldar, A. and F. J. Miller. 1982. Penetration Depth in Concrete for Nondeformable Missiles. *Nucl Eng. Des.* 71: 79-88.
- [6] Forrestal, M. J., K. Okijima, and V. K. Luk. 1988. Penetration Aluminium Targets with Rigid Long Rods. *Trans. ASME J. Appl. Mech.* 55: 755-760.
- [7] Forrestal, M. J., N. S. Brar, and V. K. Luk. 1989. Penetration of Strain-hardening Targets with Rigid Spherical-nose Rods. *Computational Techniques for Contact, Impact, Penetration and Perforation of Solids.* AMD-Vol. 103: 215-222.
- [8] Forrestal, M. J., and V. K. Luk. 1992. Penetration of 7075-T651 Aluminium Targets with Ogival-nose Rods. *Int. J. Solids Struct.* 29: 1729-1736.
- [9] Forrestal, M. J., D. J. Frew, S. J. Hanchak, and N. S. Brar. 1996. Penetration of Grout and Concrete Targets with Ogive-nose Steel Projectiles. *Int. J. Impact Eng.* 18: 465-76.
- [10] Piekutowski, A. J., M. J. Forrestal, K. L. Poormon, and T. L. Warren. 1999. Penetration of 6061-T6511 Aluminium Targets by Ogive-nose Steel Projectile with Striking Velocities Between 0.5 and 3.0 km/s. *Int. J. Impact Eng.* 23: 723-734.
- [11] Li, Q. M., S. R. Reid, H. M. Wen, and A. R. Telford. 2004. Local Impact Effect of Hard Missiles on Concrete Target. (Submitted to *Int. J. Impact Eng.*).
- [12] Chen, E. P. 1990. Finite Element Simulation of Perforation and Penetration of Aluminum Targets by Conical-nosed Steel Rods. *Mech. Mater.* 10: 107-115.
- [13] Chen, E. P. 1995. Numerical Simulation of Penetration of Aluminum Targets by Spherical-nose Steel rods. *Theoretical and Applied Fracture Mechanics.* 22: 159-164.
- [14] Peric, D., C. H. Hochar, M. Dutko, and D. R. J. Owen. 1996. Transfer Operator for Evolving Meshes in Small Strain Elasto-plasticity. *Comput. Method Appl. Mech. Engn.* 137: 331-344.
- [15] Peric, D., M. Vaz, Jr., and D. R. J. Owen. 1999. On Adaptive Strategies for Large Deformations of Elasto-Plastic Solids at Fine Strains: Computational Issue and Industrial Application. *Comput. Method Appl. Mech. Engn.* 176: 279-312.
- [16] Warren, T. L., and M. R. Tabbara. 2000. Simulations of the Penetration of 6061-T6511 Aluminum Targets by Spherical-nosed VAR 4340 Steel Projectiles. *Int. J. Solids Struct.* 37: 4419-4435.
- [17] Chen, X. W., and Q. M. Li. 2002. Deep Penetration of a Non-deformable Projectile with Different Geometrical Characteristics. *Int. J. Impact Eng.* 27: 619-37.